

Optical Chemical Sensors for Soil Analysis: Possibilities and Challenges of Visualizing NH₃ Concentrations as well as pH and O₂ Microscale Heterogeneity

Theresa Merl¹, Yihuai Hu², Johanna Pedersen², Silvia E. Zieger¹, Marie Louise Bornø³, Azeem Tariq^{3,4}, Sven Gjedde Sommer², Klaus Koren^{1*}

¹ Aarhus University Centre for Water Technology, Department of Biology, Section for Microbiology, Aarhus University, Ny Munkegade 114, 8000 Aarhus C, Denmark

² Department of Biological and Chemical Engineering, Aarhus University, Gustav Wieds Vej 10, 8000 Aarhus C, Denmark

³ Department of Plant and Environmental Sciences, University of Copenhagen, Thorvaldsensvej 40, 1871 Frederiksberg, Denmark

⁴ School of Environmental Sciences, University of Guelph, Ontario N1G2W1, Canada

*Correspondence klaus.koren@bio.au.dk;

Keywords: Ammonia, Optode, Soil Oxygen, Soil pH, Soil Water Content, Dairy Sludge, Microenvironment

ABSTRACT: Agricultural nitrogen (N) application to soils is the main source of atmospheric ammonia (NH₃) emissions. Ammonia negatively impacts the environment on a large scale. These emissions are affected by spatiotemporal heterogeneities of parameters within the soil on a microscale. Some key parameters controlling processes of the N cycle are soil oxygen (O₂) and pH. To better understand biogeochemical soil processes and NH₃ emissions we propose the application of optical chemical sensors (optodes) in soils. The use of optodes in soil science is in its infancy. In this study, we investigated the possibilities and challenges of using optodes in non-waterlogged soils with the extended application of a recently developed NH₃ optode in combination with pH and O₂ optodes in two different soils and with different fertilizers. Our results demonstrated the possibility to visualize reductions of NH₃ concentrations by 76 % and 87 % from the incorporation of sludge compared to the surface application of sludge. We showed in 2D how soil pH and fertilizer composition correlate with NH₃ volatilization. Our measurements revealed that pH optodes show certain advantages over conventional methods when measuring pH in soils *in-situ*. Lastly, we investigated spatiotemporal dynamics of O₂ at

34 different soil water contents and discussed potential challenges, which can lead to measuring
35 artifacts.

36

37 INTRODUCTION

38

39 Soils facilitate life and feed the world population as they are the fundament for healthy
40 ecosystems and food production¹. Soils are complex biological systems due to their high
41 biogeochemical activity and spatiotemporal heterogeneities. Distinct physical, chemical, and
42 biological soil properties create microsites within the soil matrix. These sites are involved in
43 important soil processes including both nutrient cycling and gas formation, as they are highly
44 influenced by soil heterogeneity²⁻⁵.

45 In agricultural soils, fertilization and soil amendments affect the soil composition as well
46 as soil properties. Different fertilizer management strategies may cause variations of soil pH,
47 substrate availability, and O₂ within the soil matrix. Within the soil, the production and
48 formation of ammonia (NH₃) are highly sensitive to changes in soil parameters such as soil
49 moisture, pH, O₂, and different nitrogen (N) forms^{5,6}. During the last century, N fertilizers have
50 been applied excessively to agricultural soils, thereby increasing the emissions of reactive N
51 gases (e.g., NH₃ and nitrous oxide (N₂O))⁷. Ammonia emissions from agriculture accounted
52 for 96 % of the European atmospheric NH₃ release, partly due to the low efficiency of fertilizer
53 uptake⁸. Ammonia emissions pose an environmental risk through N deposition, acidification,
54 and eutrophication⁹. Furthermore, they contribute to the formation of atmospheric particulate
55 matter (PM_{2.5}), which is associated with adverse health effects^{10,11}. Thus, there is a great
56 demand to mitigate NH₃ emissions.

57 To improve mitigation strategies, a detailed insight into local processes and interactions
58 of soil and fertilizers at microscale is needed, as this could explain the great variabilities seen in
59 NH₃ emission factors¹². Therefore, it is important to monitor concentrations of emitted NH₃ at
60 soil/air and soil/fertilizer interfaces, and at the same time continuously measure spatiotemporal
61 changes of important soil parameters in distinct microsites as these can provide a deeper
62 understanding of NH₃ emission dynamics. To date, the general approach to study soil processes
63 and gas emissions relies on bulk measurements of soil compounds and gas concentrations.
64 These bulk measurements fail to provide the spatial and temporal resolution, especially at the
65 mentioned interfaces, needed for an in-depth understanding of these complex processes. Planar

66 optical sensors, also termed optodes^{13,14}, may provide the methodological platform for high-
67 resolution spatiotemporal studies of soil processes.

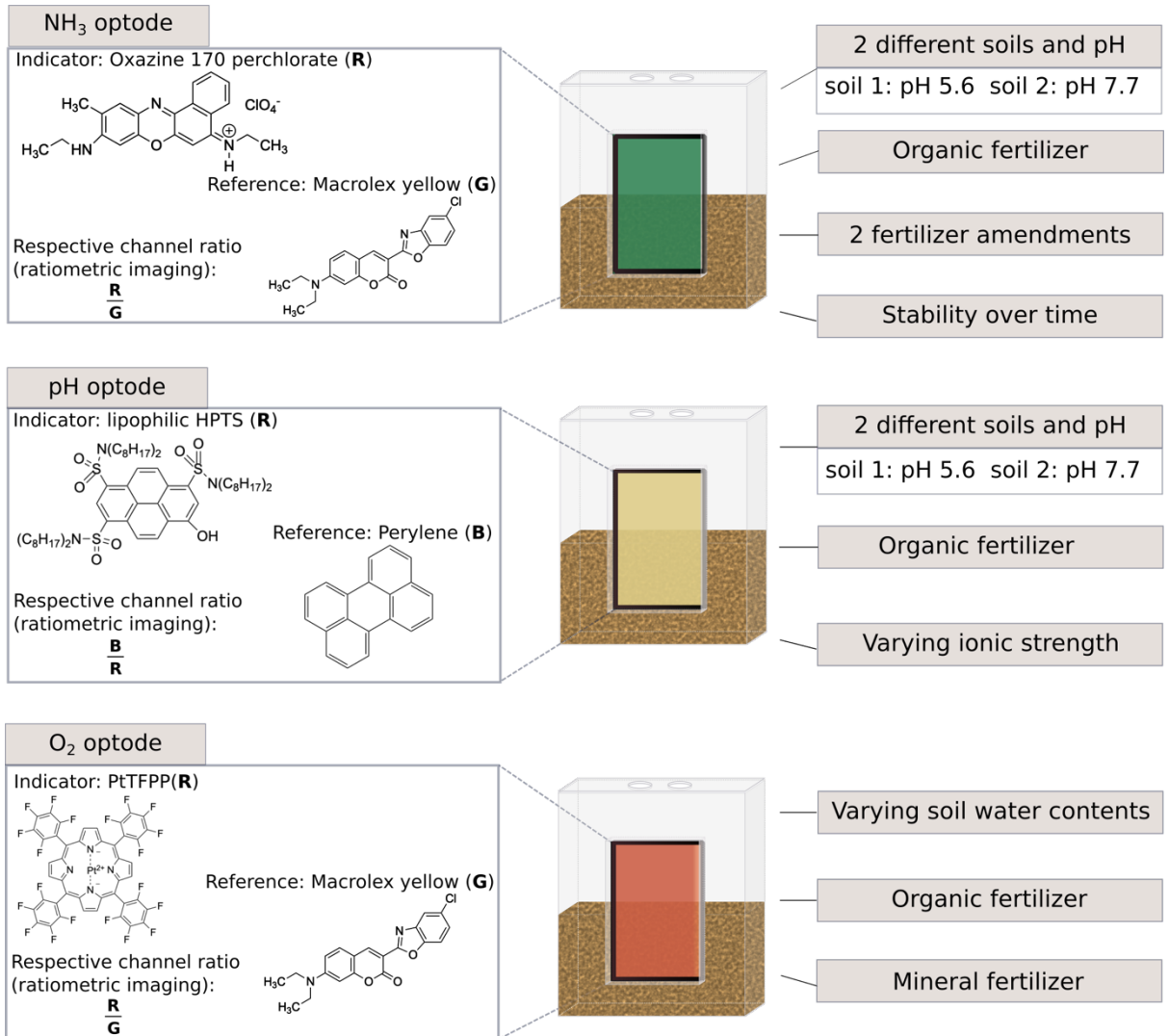
68 Optodes are reversible optical sensors that enable monitoring of variations in analyte
69 concentrations (e.g., O₂, pH, NH₃, CO₂) for several days with imaging intervals ranging from
70 seconds to hours. Thus, optodes offer non-invasive and *in-situ* imaging of analytes at high
71 spatial and temporal resolution. In short, optodes show a change in photoluminescence after
72 interacting with an analyte^{15,16}. They consist of an analyte-sensitive luminophore, which is
73 immobilized within a polymer matrix and coated onto a support material, such as a plastic foil.
74 There are two possibilities for referenced readout, which are lifetime-based, and ratiometric
75 imaging¹⁴. Optodes show great promise for studying soil biochemistry as they visualize analyte
76 changes in real time and without sample pre-treatment.

77 Some optodes, such as for pH and O₂, are well-established tools to study complex
78 environments, in particular sediments and waterlogged soils^{17,18}. However, only a few studies
79 applied optodes within non-waterlogged soils^{19,20-26}. Most relevant soil processes, from an
80 agricultural perspective, should be studied at lower water contents relevant for plant growth
81 (40-90 % of the water holding capacity (WHC)). Optodes for NH₃²⁷⁻²⁹ or NH₄⁺ are mainly
82 available for the detection of low ppb concentrations and are rarely used in soils. Therefore,
83 they are still not well characterized. Strömberg *et al.* proposed an NH₄⁺ optode that could be
84 used in soils, but despite a few studies, this optode has not been applied since^{25,30,31}. Recently,
85 we developed a dedicated NH₃ optode working in a higher concentration range²⁰. The new NH₃
86 optode is well suited for soil studies and it can be combined with other optodes to acquire
87 complex spatiotemporal patterns in 2D.

88 The objective of this study was to identify the possibilities and challenges of using
89 optodes in non-waterlogged soils and soils with different soil physico chemical characteristics.
90 Therefore, optodes for NH₃, pH and O₂ were implemented in several laboratory soil
91 experiments to assess their usability in different scenarios related to agricultural practices or
92 natural events occurring within soils (Figure 1). For this, dairy processing sludge (DPS) was
93 chosen as organic fertilizer. Dairy processing sludge is an emerging biobased fertilizer as it is an
94 organic waste product rich in phosphorus (P) and N derived from the wastewater treatment of
95 the dairy industry³². One of the reasons for its use is the goal of more sustainability for food and
96 agricultural systems³³. The soils used were two loamy sandy soils typical for Danish agricultural
97 soils and differed in their pH values. Additionally, pH optodes were tested to measure pH in

98 non-waterlogged soils *in-situ* and O₂ optodes to test the usability of such at different soil water
 99 contents.

100
 101



102
 103 **Figure 1.** Overview of the experimental set-up and utilized optodes as well as the various test scenarios.

104
 105
 106
 107
 108
 109
 110
 111
 112

113 MATERIALS AND METHODS

114 **Soil and dairy sludge.** Two soils that differ in pH were used in the different optode
115 studies (Table S1). Soil 1, a sandy loam with a high organic matter content was collected from
116 0 to 20 cm depth from an experimental field site at Aarhus University, Foulum, Denmark (56°
117 30' N, 9° 34'). The fresh soil was collected in late October 2020, passed through a 4-mm sieve,
118 and stored in a cold room (4 °C) for two weeks until the implementation of the experiment.
119 Soil 1 had a relatively low $\text{pH}_{\text{H}_2\text{O}}$ of 5.6 (Table S1). The second soil (Soil 2) was also a sandy
120 loam with a naturally high content of calcium carbonate (CaCO_3) originating from the
121 surrounding moraine. This soil was collected in February 2021 from an agricultural field located
122 in Tølløse, Zealand, Denmark (55° 37' N, 11° 48'). After collection, the soil was passed through
123 a 2-mm sieve and stored at 4 °C. This soil had a relatively high $\text{pH}_{\text{H}_2\text{O}}$ of 7.7 due to a high content
124 of CaCO_3 . The soil textures were characterized by AGROLAB Agrar/Umwelt (Sarstedt,
125 Germany). Soil pH was measured in a 1:2.5 w/w soil/water ratio and with a micro glass pH-
126 electrode (type 6.0234.110, Metrohm, Herisau, Switzerland) connected to a pH meter (type
127 764, Knick, Berlin, Germany) with a temperature probe calibrated using standard pH buffers
128 (Fluka analytical). Further soil properties were analyzed and details can be found in the
129 Supporting Information (SI). Soil properties of soil 1 and soil 2 are listed in Table S1.

130 DPS was obtained from a wastewater treatment plant of a dairy production factory in
131 Videbæk, Denmark. It was stored at -18 °C until three days prior to the start of the experiment.
132 The chemical properties of DPS were measured by an accredited laboratory (Højvang
133 laboratorier A/S, Denmark). Properties of the DPS are presented in Table S1.

134 **Experimental setup for NH_3 , pH and O_2 measurements.** A total of five studies were
135 conducted to elucidate different aspects of implementing optodes in soil studies using different
136 N fertilizers, optode combinations, soil types, and water contents. An overview of the different
137 studies can be found in Table 1, and Figure 1. For the experimental setup specially designed
138 transparent plastic chambers with removable front walls and lids were used as measurement
139 chambers (L x W x H: 60 x 39 x 100 mm) (Figure 1 & Figure S2). Soil and fertilizers were
140 incubated in the chambers, while optodes were fixed on an integrated glass window (50 x 50
141 mm) equipped on the front walls.

142 In all five studies (Table 1), the soils were packed into the chambers achieving a soil
143 bulk density of 1.3 g cm^{-3} resembling field soil bulk density. The soil packing method was
144 adopted from Zhu et al.³⁴ and Nguyen et al.³⁵. In studies using Soil 1, the chambers were packed

145 to 36 mm depth, and in studies with Soil 2, the chambers were packed to 38 mm depth, thus
146 both the soil and the air above could be investigated through the optode window. The
147 gravimetric soil water contents in studies 1-4 were kept at 35 %, which corresponds to 80 % and
148 93 % of WHC for soils 1 and 2, respectively. This water content resembles moist non-
149 waterlogged field soil. In all studies the chambers were closed on top with a lid to ensure the
150 soil water content remained constant.

151 In Studies 1-4, DPS was applied either in the middle of the soil (SM) or on top of the
152 soil (ST) to monitor the differences in NH₃ emissions, pH, and in one case O₂ from these two
153 treatments applied on the two different soils. The middle layer with DPS was a hotspot of
154 soil/sludge mixture where 5 % and 4.4 % (w/w) DPS were applied on a dry matter basis in soils
155 1 and 2, respectively. The amount of sludge mixed into the layer was chosen to make up the air-
156 porosity volume in the soil equal to the other layers. The amounts of soil, sludge, and water
157 used for each layer can be found in the Supporting Information (SI). In the ST treatments the
158 same amount of DPS that was used to mix in the SM treatments was simply applied in a layer
159 on top of the soil. Control chambers with no DPS amendment were included in all studies.

160 In order to investigate the difference in O₂ level at one constant gravimetric soil water
161 content (35%) with DPS, one chamber was also equipped with an O₂ optode in study 1 using
162 soil 1 and applying the sludge in the middle (SM). This was compared to study 5. In Study 5,
163 the use of O₂ optodes under different gravimetric soil water contents relevant for plant growth
164 was investigated. Three different gravimetric water contents of 18 %, 25 % and 32 %
165 corresponding to 41 %, 57 % and 73 % of WHC designated as low (L), medium (M), and high
166 (H) water content, respectively, were included. This investigation was included to describe the
167 more general use of optodes under agricultural relevant water contents. The chambers were
168 filled with soil 1 and packed in the same way as described above, however, varying amounts of
169 water were added. Instead of sludge 750 mg of mineral fertilizer (calcium ammonium nitrate,
170 CAN, Yara), equivalent to 101.25 mg NH₄-N, were distributed on top. Furthermore, rain was
171 simulated by adding equal amounts of water to each chamber to raise the water contents by 11
172 %, which equals a 4.67 mm rain event. This altered the soil water contents to 29 % (Rain-L),
173 36 % (Rain-M), and 43 % (Rain-H), respectively.

174 **Planar optode fabrication.** Optodes for NH₃ were prepared as previously reported by
175 Merl & Koren²⁰ and so were optodes for O₂ and pH^{20,36}. A detailed description of the
176 preparation steps can be found in the Supporting Information (SI).

177 **Imaging setup and measurement.** In studies 1 and 2 the imaging setup consisted of a
178 SLR camera (EOS 1300D, Canon, Japan) combined with a macro-objective lens (Zoom lens
179 EF-S18-55mm f/3.5-5.6 III, Canon, Japan), a yellow 455 nm long-pass filter (GG455
180 SCHOTT, 52 mm x 2 mm) with another plastic filter (#10 medium yellow; LEEfilters.com).
181 The plastic filter was mounted in front of the long-pass filter to regulate background
182 fluorescence. A 405 nm UV LED (r-s components, Copenhagen, Denmark) paired with a short-
183 pass filter (Hoya B-390 HFB 3925, UQG Optics, Cambridge, England) was used to excite the
184 optodes. The LED, which functions as the flashlight, was controlled with a trigger box. This
185 box is a USB-controlled LED driver unit (imaging.fish-n-chips-de) and is operated by the
186 Look@RGB (imaging.fish-n-chips-de) software, which also enables the gathering of the sample
187 images and simultaneously operates the SLR camera and LED.

188 In Studies 3 and 4 the imaging setup differed in the SLR camera, which had the near-infrared
189 filter removed (EOS 1300D, Canon, Japan), and a macro-objective lens (Macro 100 F2.8 D,
190 Tokina, Japan), as well as an orange 530 nm long-pass filter (OG530 SCHOTT, 52 mm x 2
191 mm). Instead of an UV LED, a blue LED (470 nm) together with a short-pass filter (Dichroic
192 blue filter CDB-2511, UQG Optics, Cambridge, England) was used (Figure S1).

193 Calibrations were conducted prior to each experiment using the exact same setup as
194 consecutively used in the respective experiment. Calibrations and data analysis for NH₃, O₂ and
195 pH optodes were conducted as described by Merl & Koren²⁰ and previous studies³⁶⁻³⁸. In terms
196 of the NH₃ optodes, it is important to emphasize that these were wet calibrations. The
197 measured ratios from the optodes were translated into ppm as a mass fraction from mg L⁻¹ as a
198 result of the wet calibration. In order to assess the relative differences in NH₃ concentrations
199 between treatments, the wet calibration was applied to the gas phase measurements. This is the
200 fastest and simplest procedure at this point.

201 In each study, images were taken every 10 minutes for the first hour, and then the interval was
202 increased to an image every hour, then to an image every two hours, up to an image every three
203 hours. In total images were acquired for a total of 21 hours for all studies except the studies
204 using O₂ optodes, in these long-term imaging was conducted for 7 days and up to 18 days.

205
206
207

208
209

Table 1: Overview of Studies 1-5 using ammonia (NH₃), pH and oxygen (O₂) optodes. Properties of the soils and DPS can be found in Table S1. DPS: dairy processing sludge.

	Study 1	Study 2	Study 3	Study 4	Study 5
Soil	Soil 1	Soil 2	Soil 2	Soil 2	Soil 1
Soil pH	5.6	7.7	7.7	7.7	5.6
Fertilizer type	DPS	DPS	DPS	DPS	Mineral fertilizer
Fertilizer application	Middle	Middle	Top & middle	Top & middle	Top
Duration	21 h/ 18 d	21 h	21 h	21 h	7 d
Gravimetric water content (%)	35	35	35	35	18, 25, 32
% of WHC	80	93	93	93	41, 57, 73
Optodes	NH ₃ , pH/ O ₂	pH	NH ₃	NH ₃	O ₂

210

211

212 **RESULTS AND DISCUSSION**

213 In terms of agricultural practices, the main aim is to adjust fertilizer management in a
214 way that most of the applied N is utilized by the crops and to mitigate N loss (e.g. via NH₃ or
215 N₂O emissions). Hence, NH₃ concentrations resulting from varying fertilizer amendments were
216 investigated with NH₃ optodes to assess the optodes' applicability as a screening method. Due
217 to the interdependencies of NH₃ emissions with soil O₂ and pH, we also tested optodes for
218 these analytes in similar settings as those chosen for the NH₃ optodes. These settings comprised
219 non-waterlogged soils and the same organic fertilizer (DPS). Due to the higher dry matter
220 content of DPS compared to manure it was possible to keep the soil non-waterlogged while
221 using an organic fertilizer. Below, we show the findings of the usability of optodes in agricultural
222 settings and non-waterlogged soils.

223

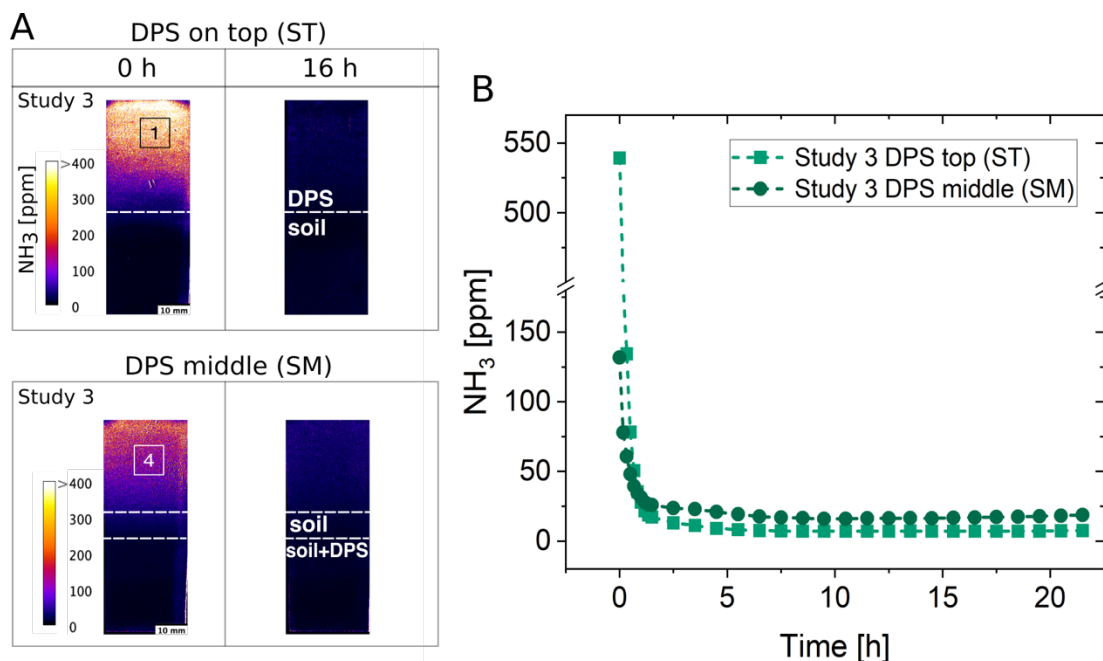


Figure 2. A: False color images showing the NH₃ concentrations of study 3 with the treatment organic fertilizer (DPS) on top (ST) and in the middle (SM). These false color images are examples from the start (0 h) and from a timepoint at 16 h. The dotted lines indicate where the soil and the mixture of soil and slurry interphase start. B: NH₃ concentrations from the regions of interest (ROIs) 1 and 4 as can be seen in A over a period of 20 h.

Ammonia optode performance in different soils and DPS application strategies.

The possibility to monitor differences in NH₃ concentrations with optodes from dairy sludge (DPS) applied on top of the soil (ST) and from DPS incorporated into the middle of the soil (SM) was tested. This was done in Study 3 and 4 using soil 2 with pH 7.7 and adjusting the gravimetric soil water content to 35%. Examples of images and the concentration change over time are shown in Figure 2 for the NH₃ optode from Study 3. Regions of interest (ROIs) were chosen to represent the headspace above the soil and to illustrate differences in NH₃ dynamics. Higher NH₃ concentrations above the soil resulted from the ST treatment compared to the SM treatment. The results from Study 4 show the same pattern and can be found in the SI (Figure S5). In both treatments a sudden spike in NH₃ concentration can be seen immediately after sludge application. The NH₃ concentration was four times higher in the ST treatment than in the SM treatment in Study 3 and around seven times higher in Study 4 (Figure S5). Differences in the NH₃ concentrations between Study 3 and 4 could be due to a slight difference in the thawing and handling of the DPS in the experimental setup. In Study 4 the DPS was not completely thawed at the time of application, thus, infiltration differences of the sludge could have occurred as it is assumed that the more liquid (completely thawed) the fertilizer the faster the infiltration of such, resulting in lower NH₃ concentrations. The incorporation of sludge (SM) led to reductions of NH₃ concentrations by 76 % and 87 % in Studies 3 and 4, respectively, compared to the surface application of sludge (ST). These values of reduction in NH₃ concentration are within the range reported by Monaco *et al.* for a laboratory scale experiment investigating the NH₃ reduction from the incorporation of pig slurry compared to surface-applied slurry, which yielded a 81.7 % reduction in NH₃³⁹. In field studies with the same objective reductions in NH₃ of 40-60 %⁴⁰ and 80 %⁴¹ were reported. Additionally, the

253 immediate high NH_3 concentrations resulting from the surface application of fertilizer were
254 also observed in laboratory scale experiments³⁹ as well as in field studies⁴⁰. Upon the immediate
255 NH_3 release a decline in NH_3 concentrations followed for about two hours. These
256 concentration profiles over time were also seen in previous studies^{20,39}, and thus results from
257 the NH_3 optodes follow the general expected trend. Lower NH_3 concentrations in the
258 treatments with sludge applied in the middle are observed due to the soil creating a barrier,
259 which induces a complete air-side resistance⁴².

260 These NH_3 concentrations are not to be considered as absolute values but rather as a
261 method to assess relative differences between treatments. There are two reasons for that.
262 Firstly, we observed that the wet calibration is not directly applicable to the gas phase
263 concentrations due to changes in humidities and because the newly developed NH_3 optodes
264 are humidity dependent (e.g. the concentration measurements vary with humidity). The
265 humidity dependency of the NH_3 optodes as well as the need to calibrate in the gas phase are
266 not yet fully explored and need further investigations. Secondly, the chambers were kept closed
267 while imaging NH_3 in the attempt to have well-defined soil system boundaries and thus
268 eliminate the need to account for fluxes of energy and matter¹. However, the emission of NH_3
269 is mainly restricted by the air-side resistance⁴², therefore, chambers without a continuous air-
270 flow will restrain the NH_3 emission due to an increased laminar film boundary while an
271 increased gas-phase NH_3 concentration is obtained compared to natural field conditions⁴³.

272 The impact soil pH has on NH_3 concentrations is shown in Figure 3. In three studies
273 sludge with a pH of 7.8 was applied into the middle of soils with different pH values. In Study
274 1 soil with a pH of 5.6 (Soil 1) and in Studies 3 and 4 soil with a pH of 7.7 (Soil 2) was used.
275 The pH-dependent equilibrium of NH_3 and NH_4^+ causes $\text{NH}_3\text{-N}$ to be mostly present as NH_4^+
276 (100%) at pH 6, whereas an increase to pH 8 results in a shift where both forms NH_4^+ (90%)
277 and NH_3 (10%) are present (Figure 3A). This seemingly small shift in pH resulted in two and
278 six times higher NH_3 concentrations above the soil in Study 3 and 4, respectively, compared to
279 Study 1 (Figure 3B). The low pH soil (Soil 1) must have buffered the pH of the sludge, which
280 was higher than the soil, and this resulted in lower NH_3 concentrations compared to the
281 amendment of the same sludge in Soil 2. These results emphasize the importance of the
282 chemical microenvironment of the soil on NH_3 emissions. Therefore, it can be an advantage to
283 employ optodes for NH_3 and pH simultaneously as they can depict these interdependent and
284 important processes further and on a high spatiotemporal scale.

285
286

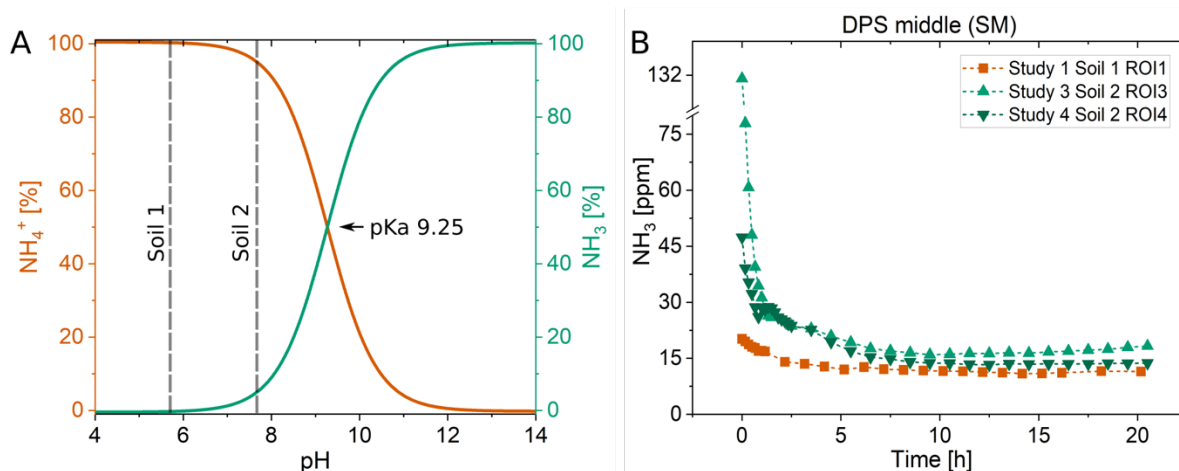


Figure 3. A: The pH-dependent equilibrium between ammonium (NH₄⁺) and ammonia (NH₃) where the dotted lines show the pH the two soil samples (soil 1 and soil 2) had. B: NH₃ concentrations of the regions of interest (ROIs) taken from the air interphase above the soil from each study (study 1, 3 and 4) over a period of 20 hours in order to show NH₃ emission from soil 1 and soil 2 with the treatment (SM) organic fertilizer (dairy sludge) amended in the middle.

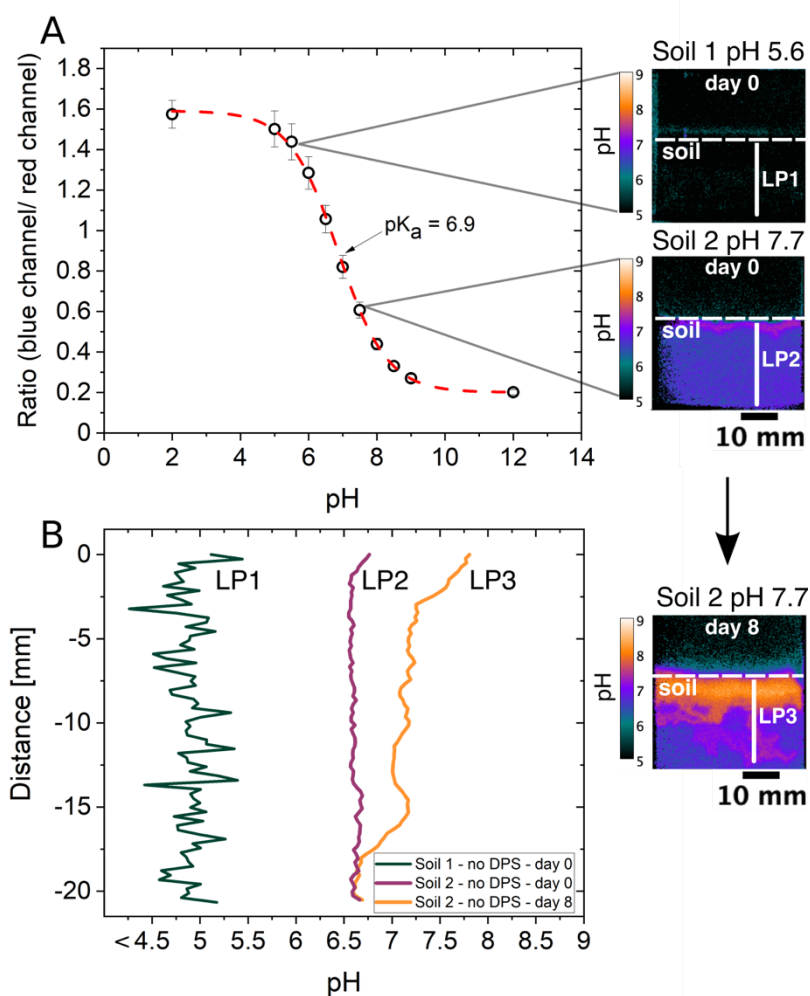
287
288
289
290
291
292

293
294

Using optodes to measure spatiotemporal variations in soil pH. Soil pH is a key parameter in soil fertility, as it controls redox reactions, nutrient and toxin bioavailability, and affects important biological processes^{44,45}. This makes soil pH a parameter of general importance, and *in-situ* and constant monitoring will contribute to a better understanding of the complexity of soils. Traditionally, soil pH is assessed with conventional laboratory pH measuring methods utilizing potentiometric pH electrodes (in aqueous or mild saline extracts)⁴⁴. While pH glass electrodes are fast and cover a wide pH range, they can only measure bulk pH in samples where the soil-to-solution ratio is changed to unnatural ratios⁴⁶. Therefore, *in-situ* pH measurements at the soil's native gravimetric soil water content or spatially resolved measurements are not possible. This way hotspots of pH changes can not be determined in a complex system such as soil. Optical sensors for pH, on the other hand, can be used *in-situ*, without the need of sample extraction, and can therefore unravel the spatial and temporal pH heterogeneities of soils⁴⁴. However, both methods have their limitations regarding precise pH measurements, which come from different non-thermodynamic assumptions inherent in their modes of operation⁴⁷. Due to that, an important differentiation between optical pH sensing and potentiometric pH measurements needs to be considered, which is that optical pH sensors base pH measurements on the concentration of a pH-sensitive dye, whereas pH is measured as activity of hydrogen (H⁺) ions in the potentiometric approach^{46,47}. The latter is also known as the definition of pH in solution but soils can not always be in solution if the pH needs to be assessed in a non-waterlogged state. Soil ionic strength is another example that contributes to biased pH measurements and is a soil parameter of great importance known to have large variances⁴⁸. Even though also optical pH sensors show cross-sensitivity to ionic strength the effect can be rather small⁴⁹. A minimal effect of ionic strength on the response can be achieved, especially by using non-charged pH-sensitive dyes⁴⁹ as the one used in the pH optodes described in this study. The diminished impact different ionic strengths have on the used pH

318

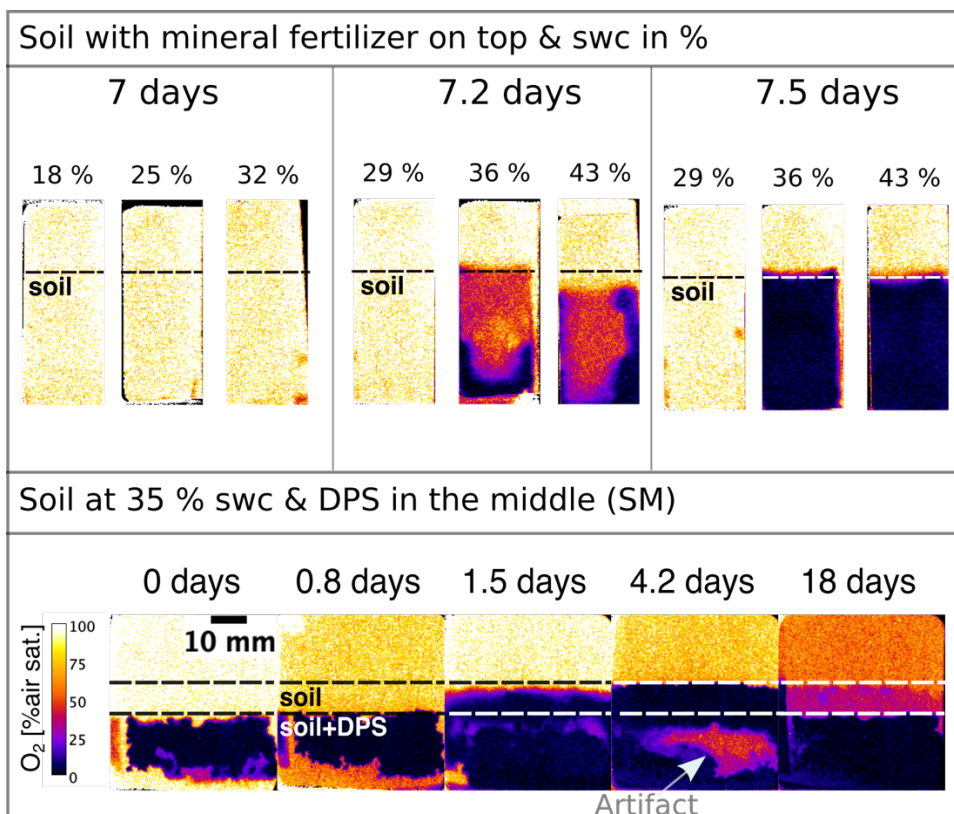
319 optode is illustrated in Figure S6 and shows the slight differences in ratios at the same pH values
 320 but with three different IS (IS 0.10, 0.38 and 1.00 M).
 321



322 **Figure 4.** A: pH calibration curve showing the pK_a of the respective pH optode and the dynamic range. Error bars depict the
 323 minima and maxima of the chosen regions of interest for each calibration step. B: Line profiles resulting from study 1 using soil
 324 1 (pH 5.6) and study 2 using soil 2 (pH 7.7), where no sludge was added in either of the shown images.
 325

326
 327 Despite the advantages optical pH sensors bring to soil analysis they have not been used
 328 extensively in non-waterlogged soils so far. To expand beyond current approaches, we wanted
 329 to investigate the applicability of pH optodes in soils with lower soil water contents than in
 330 completely waterlogged soils, as waterlogged soils are not appropriate to study most relevant
 331 soil processes. We adapted the water content of both soils to 35 %, corresponding to 93 % of
 332 water holding capacity, which is a relevant water content when considering agricultural
 333 production. Here we show that pH optodes are indeed suited for soils with lower soil water
 334 content when considering some of the optical sensor's limitations. Figure 4A depicts a pH
 335 optode calibration curve with the dynamic range being between pH 5.5 to pH 8.5 and where
 336 the two soil samples' pH values are located within that range. While potentiometric pH sensors
 337 cover a wide pH range, optical pH sensors only cover a range of maximally 3 pH units, but their
 338 accuracy is superior to the potentiometric pH sensor within the sensitive range⁴⁶. The highest

339 sensitivity of a pH-sensitive indicator dye is reached at $\text{pH} = \text{pK}_a$, and the limitation of the pH
 340 range is attributed to $\text{pH} = \text{pK}_a \pm 1.5$. Monitoring the pH works well in a non-waterlogged soil
 341 sample if the soil pH is well within the range of the sensor as seen in Figure 4A for Soil 2 but
 342 not so well if a soil sample is just at the edge of that range as seen for Soil 1 (Figure 4A). A
 343 reason for the possibility to measure pH even in samples that are non-waterlogged can be the
 344 polymer used to immobilize the pH indicator dye in. The optical sensor in this study was
 345 prepared with a hydrogel (Hydromed D4), which is known to have a water absorption
 346 characteristic of 50 %⁵⁰. The polymer absorbs water present in the sample and swells, which is
 347 an advantage in facilitating proton exchange and detection even at relatively low soil water
 348 contents.



350 **Figure 5. A:** False color images of the oxygen (O_2) concentration from Study 5 upon synthetic fertilizer was added and the
 351 images were taken for 7 days at the three different soil water contents (swc) (18 %, 25 % and 32 %) showing one of two
 352 replicates per soil water content. The image at the timepoint 7.2 days was taken after 11.5 mL of water was added to simulate
 353 a rain event. This heightened the soil water contents to 29 %, 36 % and 43 %. Only 8 hours (7.5 days) later the third panel
 354 shows the chambers with soil water contents of 36 % and 43 % with anoxic zones. Additionally, the false color images of the O_2
 355 concentration of Study 1 are shown. In this study a soil water content of 35% was maintained and organic fertilizer was applied
 356 in the middle part of the packed soil. Imaging was conducted for 18 days.

358
 359 As soon as the soil's pH value is outside of the dynamic range the false color image in
 360 Figure 4A as well as the line profile 1 (LP1) from Soil 1 in Figure 4B show that it is not possible
 361 to achieve proper pH measurements. LP1 shows a rather noisy signal due to reaching the
 362 detection limit of the pH optode while LP2 and LP3 from Soil 2 result in much better signal
 363 qualities as they lie well within the dynamic range. This shows that it is important to consider
 364 the optical sensor's working range and to investigate the soil system's characteristics in advance.

365 Despite the proposed considerations that need to be taken into account before using optical
366 sensors for soil pH analysis we still think it is a good approach for *in-situ* measurements at lower
367 soil water contents. A study by Nielsen *et al.* found that the conventional laboratory pH
368 measurements for soils with suspension samples continuously overestimated the pH compared
369 to *in-situ* pH measurements directly in the field⁵¹. The *in-situ* pH values were 0.5-0.8 pH units
370 lower than the pH values measured with the extraction method in the laboratory. A similar
371 trend was observed in our studies too. The soils used in the present study were also measured
372 in a soil water suspension (soil:deionized water 1:2.5 w/w) resulting in a soil pH of 5.6 (Soil 1)
373 and a soil pH of 7.7 (Soil 2). The *in-situ* measurements with the pH optodes, however, revealed
374 a soil pH of around pH 5 for Soil 1 and a soil pH of pH 6.6 for Soil 2. This reveals lower pH
375 measurements with the pH optodes here too, with a difference of 0.6 units for Soil 1 and 1.1
376 units for Soil 2. Possible reasons for the higher pH values measured with the standard laboratory
377 method could be the different modes of operation⁴⁷, the release of buffering ions from soil biota
378 due to drying, extracting, and rewetting of soil samples⁵¹ or the change in electrolyte
379 concentration due to dilution of the soil with water. Hence, it should become more common
380 practice to choose *in-situ* pH measurements over the standard method to avoid sample handling
381 artifacts.

382 **Oxygen optodes in non-waterlogged soils.** *In-situ* measurements of soil O₂ contents
383 with optical sensors have been investigated in a number of studies, especially in combination
384 with amendments of organic fertilizers^{19,23,24}. That is because the availability and spatial
385 distribution of O₂ have immense impacts on C and N cycling as well as greenhouse gas
386 emissions. However, most of these studies were conducted in soils with high soil water
387 contents, partly due to the addition of liquid manure as organic fertilizer. In the present study,
388 we investigated the useability of O₂ optodes related to the difference in O₂ distribution in soils
389 with different gravimetric soil water contents and added a mineral and an organic fertilizer
390 (Figure 5). It can be seen in Figure 5 that oxic conditions dominated for the first seven days
391 after mineral fertilizer was applied to the top of the soil. In contrast, O₂ depletion zones
392 immediately formed when organic fertilizer was applied and mixed within the middle area of
393 the soil, which is due to the more easily biodegradable organic C in the sludge stimulating
394 greater microbial activity. The O₂ depletion zones expanded to the surrounding soil for the next
395 days. On day 4 a small zone of O₂ increase can be seen within the sludge and soil band (Figure
396 5, bottom). It looks like O₂ production took place. This, however, is very unlikely as there were
397 no plants and therefore plant roots involved in this sample to explain such a rise in O₂ levels.
398 More likely though is the detachment of soil from the optode and O₂ influx from the headspace
399 to that area. This points out how important it is that the sample is in good contact with the
400 optode in order to not misinterpret measured artifacts.

401 Another challenge that is presented here is the measurement of O₂ dynamics at different
402 soil water contents. This can be seen in Figure 5 in the treatment with mineral fertilizer on top
403 where the soil with gravimetric water contents from 18-32 % is fully oxygenated. And only after
404 increasing the soil water content to 36 % and 43 % an anoxic zone within the soil is formed.
405 This supports the fact that O₂ diffusion becomes limited as soon as the soil becomes more
406 waterlogged. It also shows that air filled pore spaces filled up with water after irrigation, which

407 supports the increase of the anoxic area. Even though O₂ optodes show a fully oxygenated soil
408 under certain soil water contents it does not necessarily mean that the oxygen concentrations
409 shown with this measurement method depict the whole complexity of the O₂ dynamics. Anoxic
410 zones can be present within soil particles, as shown by Revsbech *et al.*⁵² by using a Clark-type
411 microsensors for O₂ within small soil particles. Even though optodes offer a high-resolution
412 measurement together with the possibility of imaging heterogeneities, it also showcases the
413 limitations of this method as it is a bulk measurement compared to even higher resolution
414 methods like microsensors. This together with the need for contact between sample and optode
415 are not necessarily shortcomings of O₂ optodes in soils but rather challenges that need to be
416 considered when designing the study.

417 **Considerations when using optodes in non-waterlogged soils.** Overall, the studies
418 show that optodes can be a valuable additional tool in the soil analysis toolbox due to their
419 abilities and the possibility to combine them in the same system if their limitations are taken
420 into consideration. Our results demonstrated the ability to visualize the relative differences in
421 NH₃ concentrations resulting from varying fertilizer amendments and from different soil pH
422 values. On a large scale such changes in concentration could have a big effect. Hence, the
423 advantage of such short-term experiments can be to offer a preliminary assessment of the
424 impact new fertilizers, application techniques and soil-fertilizer interactions could mean on a
425 bigger scale. Therefore, a fast information transfer can be offered due to the reduction of
426 laborious and costly field experiments for soil and fertilizer analysis with high spatiotemporal
427 resolution. The interpretations of the NH₃ optode results, though, still need to be considered
428 as relative values due to a possible humidity dependency and needed calibration improvements
429 to allow more accurate gas phase measurements. Our measurements showed that pH optodes
430 are a great alternative to conventional methods when it comes to measuring pH in soils *in-situ*.
431 Additionally, it is important to be aware of the diminished dynamic range pH optodes operate
432 in compared to potentiometric sensors. In regards to O₂ optodes, we showed that it is not
433 always feasible to measure spatiotemporal dynamics of O₂ if soil water contents are too low.
434 The settings of the biological system need to be considered first regarding soil water content,
435 organic matter, and processes that might occur. Another aspect regarding all optodes is their
436 temperature dependency, which is predictable and can be corrected for⁵³ or circumvented by
437 keeping the temperature stable throughout laboratory-based experiments. Showcasing the
438 possibilities as well as the challenges of optodes in soil systems could aid to bridge the gap
439 between two fields. This will help to broaden our understanding of complex soil processes and
440 how these are linked to emissions from the agricultural sector by adding missing links of
441 spatiotemporal variations within the soil and at the soil/air interphase.

442
443
444
445
446
447
448

449 **ACKNOWLEDGEMENT**

450 This study was supported by research grants from the Poul Due Jensen Foundation (KK), a
451 Sapere Aude grant from the Independent Research Fund Denmark (IRFD): DFF-8048-
452 00057B (KK), a Green Development and Demonstration Program (GUDDP) from the Ministry
453 of Food, Agriculture and Fisheries of Denmark (journal nr.: 34009-21-1829), and the European
454 Union's Horizon 2020 Marie Skłodowska-Curie Actions (MSCA) Innovative Training
455 Networks (ITN) (No. 814258). The authors want to thank Lars Borregaard Pedersen and
456 Mette L. G. Nikolajsen for excellent technical support.

457
458

459

460 **REFERENCES**

461

- 462 (1) Strawn, D. G.; Bohn, H. L.; O'Connor, G. A. *Soil Chemistry*, Fourth Edi.; John Wiley &
463 Sons, Ltd: The Atrium, Southern Gate, Chichester, West Sussex, PO19 8SQ, UK,
464 2015.
- 465 (2) Nunan, N.; Schmidt, H.; Raynaud, X. The Ecology of Heterogeneity: Soil Bacterial
466 Communities and C Dynamics. *Philos. Trans. R. Soc. B Biol. Sci.* **2020**, 375 (1798).
467 <https://doi.org/10.1098/rstb.2019.0249>.
- 468 (3) Smith, K. A. Changing Views of Nitrous Oxide Emissions from Agricultural Soil: Key
469 Controlling Processes and Assessment at Different Spatial Scales. *Eur. J. Soil Sci.* **2017**,
470 68 (2), 137–155. <https://doi.org/10.1111/ejss.12409>.
- 471 (4) Wilmoth, J. L. Redox Heterogeneity Entangles Soil and Climate Interactions. *Sustain.*
472 **2021**, 13 (18). <https://doi.org/10.3390/su131810084>.
- 473 (5) Cameron, K. C.; Di, H. J.; Moir, J. L. Nitrogen Losses from the Soil/Plant System: A
474 Review. *Ann. Appl. Biol.* **2013**, 162 (2), 145–173. <https://doi.org/10.1111/aab.12014>.
- 475 (6) Turner, D. A.; Edis, R. E.; Chen, D.; Freney, J. R.; Denmead, O. T. Ammonia
476 Volatilization from Nitrogen Fertilizers Applied to Cereals in Two Cropping Areas of
477 Southern Australia. *Nutr. Cycl. Agroecosystems* **2012**, 93 (2), 113–126.
478 <https://doi.org/10.1007/s10705-012-9504-2>.
- 479 (7) Zhang, X.; Davidson, E. A.; Mauzerall, D. L.; Searchinger, T. D.; Dumas, P.; Shen, Y.
480 Managing Nitrogen for Sustainable Development. *Nature* **2015**, 528 (7580), 51–59.
481 <https://doi.org/10.1038/nature15743>.
- 482 (8) Giannakis, E.; Kushta, J.; Bruggeman, A.; Lelieveld, J. Costs and Benefits of
483 Agricultural Ammonia Emission Abatement Options for Compliance with European
484 Air Quality Regulations. *Environ. Sci. Eur.* **2019**, 31 (1).
485 <https://doi.org/10.1186/s12302-019-0275-0>.
- 486 (9) Sommer, S. G.; Schjoerring, J. K.; Denmead, O. T. Ammonia Emission from Mineral
487 Fertilizers and Fertilized Crops. *Adv. Agron.* **2001**, 82 (December 2004), 557–622.
488 [https://doi.org/10.1016/s0065-2113\(03\)82008-4](https://doi.org/10.1016/s0065-2113(03)82008-4).
- 489 (10) Aneja, V. P.; Schlesinger, W. H.; Erisman, J. W. Effects of Agriculture upon the Air
490 Quality and Climate: Research, Policy, and Regulations. *Environ. Sci. Technol.* **2009**, 43
491 (12), 4234–4240. <https://doi.org/10.1021/es8024403>.
- 492 (11) Walker, J. T.; Robarge, W. P.; Shendrikar, A.; Kimball, H. Inorganic PM_{2.5} at a U.S.
493 Agricultural Site. *Environ. Pollut.* **2006**, 139 (2), 258–271.
494 <https://doi.org/10.1016/j.envpol.2005.05.019>.
- 495 (12) Hafner, S. D.; Pacholski, A.; Bittman, S.; Burchill, W.; Bussink, W.; Chantigny, M.;

- 496 Carozzi, M.; Générumont, S.; Häni, C.; Hansen, M. N.; Huijsmans, J.; Hunt, D.;
497 Kupper, T.; Lanigan, G.; Loubet, B.; Misselbrook, T.; Meisinger, J. J.; Neftel, A.;
498 Nyord, T.; Pedersen, S. V.; Sintermann, J.; Thompson, R. B.; Vermeulen, B.;
499 Vestergaard, A. V.; Voylokov, P.; Williams, J. R.; Sommer, S. G. The ALFAM2
500 Database on Ammonia Emission from Field-Applied Manure: Description and
501 Illustrative Analysis. *Agric. For. Meteorol.* **2018**, 258 (August 2017), 66–79.
502 <https://doi.org/10.1016/j.agrformet.2017.11.027>.
- 503 (13) Schäferling, M. The Art of Fluorescence Imaging with Chemical Sensors. *Angew.*
504 *Chemie - Int. Ed.* **2012**, 51 (15), 3532–3554.
505 <https://doi.org/10.1002/anie.201105459>.
- 506 (14) Wolfbeis, O. S. Materials for Fluorescence-Based Optical Chemical Sensors. *J. Mater.*
507 *Chem.* **2005**, 15 (27–28), 2657–2669. <https://doi.org/10.1039/b501536g>.
- 508 (15) Santner, J.; Larsen, M.; Kreuzeder, A.; Glud, R. N. Two Decades of Chemical Imaging
509 of Solutes in Sediments and Soils - a Review. *Anal. Chim. Acta* **2015**, 878, 9–42.
510 <https://doi.org/10.1016/j.aca.2015.02.006>.
- 511 (16) Koren, K.; Zieger, S. E. Optode Based Chemical Imaging Possibilities, Challenges,
512 and New Avenues in Multidimensional Optical Sensing. **2021**.
513 <https://doi.org/10.1021/acssensors.1c00480>.
- 514 (17) Li, C.; Ding, S.; Yang, L.; Zhu, Q.; Chen, M.; Tsang, D. C. W.; Cai, G.; Feng, C.;
515 Wang, Y.; Zhang, C. Planar Optode: A Two-Dimensional Imaging Technique for
516 Studying Spatial-Temporal Dynamics of Solutes in Sediment and Soil. *Earth-Science*
517 *Rev.* **2019**, 197 (July), 102916. <https://doi.org/10.1016/j.earscirev.2019.102916>.
- 518 (18) Koren, K.; Köhl, M. CHAPTER 7. Optical O₂ Sensing in Aquatic Systems and
519 Organisms. In *Quenched-phosphorescence Detection of Molecular Oxygen: Applications in*
520 *Life Sciences*; Papkovsky, D. B., Dmitriev, R. I. ., Eds.; Royal Society of Chemistry,
521 2018; Vol. 1, pp 145–174. <https://doi.org/10.1039/9781788013451-00145>.
- 522 (19) Zhu, K.; Ye, X.; Ran, H.; Zhang, P.; Wang, G. Contrasting Effects of Straw and Biochar
523 on Microscale Heterogeneity of Soil O₂ and PH: Implication for N₂O Emissions. *Soil*
524 *Biol. Biochem.* **2022**, 108564. <https://doi.org/10.1016/j.soilbio.2022.108564>.
- 525 (20) Merl, T.; Koren, K. Visualizing NH₃ Emission and the Local O₂ and PH
526 Microenvironment of Soil upon Manure Application Using Optical Sensors. *Environ.*
527 *Int.* **2020**, 144 (May), 106080. <https://doi.org/10.1016/j.envint.2020.106080>.
- 528 (21) Rudolph-Mohr, N.; Tötze, C.; Kardjilov, N.; Oswald, S. E. Mapping Water, Oxygen,
529 and PH Dynamics in the Rhizosphere of Young Maize Roots. *Zeitschrift für*
530 *Pflanzenernährung und Bodenkd.* **2017**, 180 (3), 336–346.
531 <https://doi.org/10.1002/jpln.201600120>.
- 532 (22) Christel, W.; Zhu, K.; Hofer, C.; Kreuzeder, A.; Santner, J.; Bruun, S.; Magid, J.;
533 Jensen, L. S. Spatiotemporal Dynamics of Phosphorus Release, Oxygen Consumption
534 and Greenhouse Gas Emissions after Localised Soil Amendment with Organic
535 Fertilisers. *Sci. Total Environ.* **2016**, 554–555, 119–129.
536 <https://doi.org/10.1016/j.scitotenv.2016.02.152>.
- 537 (23) Zhu, K.; Bruun, S.; Larsen, M.; Glud, R. N.; Jensen, L. S. Spatial Oxygen Distribution
538 and Nitrous Oxide Emissions from Soil after Manure Application: A Novel Approach
539 Using Planar Optodes. *J. Environ. Qual.* **2014**, 43 (5), 1809–1812.
540 <https://doi.org/10.2134/jeq2014.03.0125>.
- 541 (24) Van Nguyen, Q.; Jensen, L. S.; Bol, R.; Wu, D.; Triolo, J. M.; Vazifehkoran, A. H.;
542 Bruun, S. Biogas Digester Hydraulic Retention Time Affects Oxygen Consumption
543 Patterns and Greenhouse Gas Emissions after Application of Digestate to Soil. *J.*

- 544 *Environ. Qual.* **2017**, 46 (5), 1114–1122. <https://doi.org/10.2134/jeq2017.03.0117>.
- 545 (25) Delin, S.; Strömberg, N. Imaging-Optode Measurements of Ammonia Distribution
546 in Soil after Different Manure Amendments. *Eur. J. Soil Sci.* **2011**, 62 (2), 295–304.
547 <https://doi.org/10.1111/j.1365-2389.2010.01326.x>.
- 548 (26) Strömberg, N.; Engelbrektsson, J.; Delin, S. A High Throughput Optical System for
549 Imaging Optodes. *Sensors Actuators, B Chem.* **2009**, 140 (2), 418–425.
550 <https://doi.org/10.1016/j.snb.2009.05.011>.
- 551 (27) Waich, K.; Borisov, S.; Mayr, T.; Klimant, I. Dual Lifetime Referenced Trace Ammonia
552 Sensors. *Sensors Actuators, B Chem.* **2009**, 139 (1), 132–138.
553 <https://doi.org/10.1016/j.snb.2008.10.010>.
- 554 (28) Abel, T.; Ungerböck, B.; Klimant, I.; Mayr, T. Fast Responsive, Optical Trace Level
555 Ammonia Sensor for Environmental Monitoring. *Chem. Cent. J.* **2012**, 6 (1), 1–9.
556 <https://doi.org/10.1186/1752-153X-6-124>.
- 557 (29) Müller, B. J.; Steinmann, N.; Borisov, S. M.; Klimant, I. Ammonia Sensing with
558 Fluoroionophores – A Promising Way to Minimize Interferences Caused by Volatile
559 Amines. *Sensors Actuators, B Chem.* **2018**, 255, 1897–1901.
560 <https://doi.org/10.1016/j.snb.2017.08.209>.
- 561 (30) Strömberg, N. Determination of Ammonium Turnover and Flow Patterns Close to
562 Roots Using Imaging Optodes. *Environ. Sci. Technol.* **2008**, 42 (5), 1630–1637.
563 <https://doi.org/10.1021/es071400q>.
- 564 (31) Strömberg, N.; Hulth, S. An Ammonium Selective Fluorosensor Based on the
565 Principles of Coextraction. *Anal. Chim. Acta* **2001**, 443 (2), 215–225.
566 [https://doi.org/10.1016/S0003-2670\(01\)01221-1](https://doi.org/10.1016/S0003-2670(01)01221-1).
- 567 (32) Shi, W.; Healy, M. G.; Ashekuzzaman, S. M.; Daly, K.; Leahy, J. J.; Fenton, O. Dairy
568 Processing Sludge and Co-Products: A Review of Present and Future Re-Use Pathways
569 in Agriculture. *J. Clean. Prod.* **2021**, 314 (September 2020), 128035.
570 <https://doi.org/10.1016/j.jclepro.2021.128035>.
- 571 (33) European Commission. *Farm to Fork Strategy: For a Fair, Healthy and Environmentally-*
572 *Friendly Food System.*; 2020.
- 573 (34) Zhu, K.; Bruun, S.; Larsen, M.; Glud, R. N.; Jensen, L. S. Heterogeneity of O₂
574 Dynamics in Soil Amended with Animal Manure and Implications for Greenhouse Gas
575 Emissions. *Soil Biol. Biochem.* **2015**, 84, 96–106.
576 <https://doi.org/10.1016/j.soilbio.2015.02.012>.
- 577 (35) Nguyen, Q. Van; Wu, D.; Kong, X.; Bol, R.; Petersen, S. O.; Jensen, L. S.; Liu, S.;
578 Brüggemann, N.; Glud, R. N.; Larsen, M.; Bruun, S. Effects of Cattle Slurry and
579 Nitrification Inhibitor Application on Spatial Soil O₂ Dynamics and N₂O Production
580 Pathways. *Soil Biol. Biochem.* **2017**, 114, 200–209.
581 <https://doi.org/10.1016/j.soilbio.2017.07.012>.
- 582 (36) Brodersen, K. E.; Koren, K.; Moßhammer, M.; Ralph, P. J.; Köhl, M.; Santner, J.
583 Seagrass-Mediated Phosphorus and Iron Solubilization in Tropical Sediments. *Environ.*
584 *Sci. Technol.* **2017**, 51 (24), 14155–14163. <https://doi.org/10.1021/acs.est.7b03878>.
- 585 (37) Koren, K.; Moßhammer, M.; Scholz, V. V.; Borisov, S. M.; Holst, G.; Köhl, M.
586 Luminescence Lifetime Imaging of Chemical Sensors - A Comparison between Time-
587 Domain and Frequency-Domain Based Camera Systems. *Anal. Chem.* **2019**, 91 (5),
588 3233–3238. <https://doi.org/10.1021/acs.analchem.8b05869>.
- 589 (38) Larsen, M.; Borisov, S. M.; Grunwald, B.; Klimant, I.; Glud, R. N. A Simple and
590 Inexpensive High Resolution Color Ratiometric Planar Optode Imaging Approach:
591 Application to Oxygen and PH Sensing. *Limnol. Oceanogr. Methods* **2011**, 9 (SEP),

- 592 348–360. <https://doi.org/10.4319/lom.2011.9.348>.
- 593 (39) Monaco, S.; Sacco, D.; Pelissetti, S.; Dinuccio, E.; Balsari, P.; Rostami, M.; Grignani,
594 C. Laboratory Assessment of Ammonia Emission after Soil Application of Treated and
595 Untreated Manures. *J. Agric. Sci.* **2012**, *150* (1), 65–73.
596 <https://doi.org/10.1017/S0021859611000487>.
- 597 (40) Smith, K. A.; Jackson, D. R.; Misselbrook, T. H.; Pain, B. F.; Johnson, R. A. Reduction
598 of Ammonia Emission by Slurry Application Techniques. *J. Agric. Eng. Res.* **2000**, *77*
599 (3), 277–287. <https://doi.org/10.1006/jaer.2000.0604>.
- 600 (41) Sommer, S. G.; Friis, E.; Bach, A.; Schjørring, J. K. Ammonia Volatilization from Pig
601 Slurry Applied with Trail Hoses or Broadcast to Winter Wheat: Effects of Crop
602 Developmental Stage, Microclimate, and Leaf Ammonia Absorption. *J. Environ. Qual.*
603 **1997**, *26*, 1153–1160.
- 604 (42) Hudson, N.; Ayoko, G. A. Odour Sampling 1: Physical Chemistry Considerations.
605 *Bioresour. Technol.* **2008**, *99* (10), 3982–3992.
606 <https://doi.org/10.1016/j.biortech.2007.04.034>.
- 607 (43) Eklund, B. Practical Guidance for Flux Chamber Measurements of Fugitive Volatile
608 Organic Emission Rates. *J. Air Waste Manag. Assoc.* **1992**, *42* (12), 1583–1591.
609 <https://doi.org/10.1080/10473289.1992.10467102>.
- 610 (44) Nadporozhskaya, M.; Kovsh, N.; Paolesse, R. Recent Advances in Chemical Sensors
611 for Soil Analysis : A Review. **2022**.
- 612 (45) Buss, W.; Shepherd, J. G.; Heal, K. V.; Mašek, O. Spatial and Temporal Microscale PH
613 Change at the Soil-Biochar Interface. *Geoderma* **2018**, *331* (April), 50–52.
614 <https://doi.org/10.1016/j.geoderma.2018.06.016>.
- 615 (46) Steinegger, A.; Wolfbeis, O. S.; Borisov, S. M. Optical Sensing and Imaging of PH
616 Values : Spectroscopies , Materials , and Applications. **2020**.
617 <https://doi.org/10.1021/acs.chemrev.0c00451>.
- 618 (47) Janata, J. Do Optical Sensors Really Measure PH? *Anal. Chem.* **1987**, *59* (9), 1351–
619 1356. <https://doi.org/10.1021/ac00136a019>.
- 620 (48) Thomas, G. W. Soil PH and Soil Acidity G. In *Methods of Soil Analysis*; John Wiley &
621 Sons, Ltd, 1996; pp 475–490. <https://doi.org/10.2136/sssabookser5.3.c16>.
- 622 (49) Borisov, S. M.; Herrod, D. L.; Klimant, I. Fluorescent Poly(Styrene-Block-
623 Vinylpyrrolidone) Nanobeads for Optical Sensing of PH. *Sensors Actuators, B Chem.*
624 **2009**, *139* (1), 52–58. <https://doi.org/10.1016/j.snb.2008.08.028>.
- 625 (50) Hydromed <http://www.advbiomaterials.com/products/hydrophilic/HydroMed.pdf>.
- 626 (51) Nielsen, K. E.; Irizar, A.; Nielsen, L. P.; Kristiansen, S. M.; Damgaard, C.; Holmstrup,
627 M.; Petersen, A. R.; Strandberg, M. In Situ Measurements Reveal Extremely Low PH
628 in Soil. *Soil Biol. Biochem.* **2017**, *115*, 63–65.
629 <https://doi.org/10.1016/j.soilbio.2017.08.003>.
- 630 (52) Sexstone, A. J.; Revsbech, N. P.; Parkin, T. B.; Tiedje, J. M. Direct Measurement of
631 Oxygen Profiles and Denitrification Rates in Soil Aggregates. *Soil Sci. Soc. Am. J.* **1985**.
632 <https://doi.org/10.2136/sssaj1985.03615995004900030024x>.
- 633 (53) Fritzsche, E.; Staudinger, C.; Fischer, J. P.; Thar, R.; Jannasch, H. W.; Plant, J. N.;
634 Blum, M.; Massion, G.; Thomas, H.; Hoech, J.; Johnson, K. S.; Borisov, S. M.;
635 Klimant, I. A Validation and Comparison Study of New, Compact, Versatile Optodes
636 for Oxygen, PH and Carbon Dioxide in Marine Environments. *Mar. Chem.* **2018**, *207*
637 (September), 63–76. <https://doi.org/10.1016/j.marchem.2018.10.009>.
- 638